

ARTICLE



Multi-omics analyses of serum metabolome, gut microbiome and brain function reveal dysregulated microbiota-gut-brain axis in bipolar depression

Zhiming Li^{1,6,7,8,17}, Jianbo Lai^{1,2,3,4,17}, Peifen Zhang^{1,17}, Jiahong Ding^{6,7,8,17}, Jiajun Jiang¹, Chuanfa Liu^{6,7,9}, Huimin Huang^{1,5}, Hefu Zhen^{6,7,8}, Caixi Xi¹, Yuzhe Sun^{6,7,8}, Lingling Wu¹, Lifang Wang^{6,7,8}, Xingle Gao¹, Yan Li^{6,7,8}, Yaoyang Fu¹, Zhuye Jie^{6,7}, Shenghui Li¹⁰, Danhua Zhang¹, Yiqing Chen¹, Yiyi Zhu^{1,5}, Shaojia Lu^{1,2,3,4}, Jing Lu^{1,2,3,4}, Dandan Wang^{1,2,3,4}, Hetong Zhou^{1,2,3,4}, Xiuxia Yuan^{11,12}, Xue Li^{11,12}, Lijuan Pang^{11,12}, Manli Huang^{1,2,3,4}, Huanming Yang^{6,7}, Wenwei Zhang^{6,7,8}, Susanne Brix^{13,14}, Karsten Kristiansen^{6,14,15}, Xueqin Song^{11,12}, Chao Nie^{6,7,8} and Shaohua Hu^{1,2,3,4,16}

© The Author(s), under exclusive licence to Springer Nature Limited 2022

The intricate processes of microbiota-gut-brain communication in modulating human cognition and emotion, especially in the context of mood disorders, have remained elusive. Here we performed faecal metagenomic, serum metabolomics and neuroimaging studies on a cohort of 109 unmedicated patients with depressed bipolar disorder (BD) patients and 40 healthy controls (HCs) to characterise the microbial-gut-brain axis in BD. Across over 12,000 measured metabolic features, we observed a large discrepancy (73.54%) in the serum metabolome between BD patients and HCs, spotting differentially abundant microbial-derived neuroactive metabolites including multiple B-vitamins, kynurenic acid, gamma-aminobutyric acid and short-chain fatty acids. These metabolites could be linked to the abundance of gut microbiota presented with corresponding biosynthetic potentials, including *Akkermansia muciniphila*, *Citrobacter spp.* (*Citrobacter freundii* and *Citrobacter werkmanii*), *Phascolarctobacterium spp.*, *Yersinia spp.* (*Yersinia frederiksenii* and *Yersinia aleksiciae*), *Enterobacter spp.* (*Enterobacter cloacae* and *Enterobacter kobei*) and *Flavobacterium spp.* Based on functional neuroimaging, BD-related neuroactive microbes and metabolites were discovered as potential markers associated with BD-typical features of functional connectivity of brain networks, hinting at aberrant cognitive function, emotion regulation, and interoception. Our study combines gut microbiota and neuroactive metabolites with brain functional connectivity, thereby revealing potential signalling pathways from the microbiota to the gut and the brain, which may have a role in the pathophysiology of BD.

Molecular Psychiatry; <https://doi.org/10.1038/s41380-022-01569-9>

INTRODUCTION

The bidirectional interaction between the brain and the gut microbiota, the microbiota-gut-brain (MGB) axis, has emerged as a research hotspot in psychiatry. Healthy gut microbiota is essential for maintaining physical and mental well-being [1], while dysbiosis in the microbial community—imbalances in the composition and function of gut microbes—may disrupt immunological and metabolic processes [2, 3], thus reshaping host emotion, cognition, behaviour, and contribute to the pathophysiology of major psychiatric disorders [4, 5].

Bipolar disorder (BD) is a prevalent and debilitating mental illness with complex aetiology. Emerging evidence has indicated BD as a whole-body disease with changes in the gut microbiota and serum metabolome [6, 7]. Recent reviews [8, 9] have summarised evidence regarding the gut microbiota composition across major psychiatric disorders including BD, showing that higher levels of *Eggerthella*, *Lactobacillus*, *Enterococcus*, *Flavonifractor* and *Streptococcus*, and lower levels of *Coprococcus*, *Faecalibacterium* and *Ruminococcus*, were observed in BD patients compared to healthy controls (HCs). Identified bacterial genera were reported to be involved in the

¹Department of Psychiatry, the First Affiliated Hospital, Zhejiang University School of Medicine, Hangzhou 310003, China. ²The Key Laboratory of Mental Disorder's Management in Zhejiang Province, Hangzhou 310003, China. ³Brain Research Institute of Zhejiang University, Hangzhou 310003, China. ⁴Zhejiang Engineering Center for Mathematical Mental Health, Hangzhou 310003, China. ⁵Wenzhou Medical University, Wenzhou 325035, China. ⁶BGI-Shenzhen, Shenzhen 518083, China. ⁷China National GeneBank, BGI-Shenzhen, Shenzhen 518120, China. ⁸Shenzhen Key Laboratory of Neurogenomics, BGI-Shenzhen, Shenzhen 518083, China. ⁹College of Life Sciences, University of Chinese Academy of Sciences, Beijing 100049, China. ¹⁰Key Laboratory of Precision Nutrition and Food Quality, Department of Nutrition and Health, China Agricultural University, Beijing 100083, China. ¹¹Department of Psychiatry, First Affiliated Hospital of Zhengzhou University, Zhengzhou 450052, China. ¹²Biological Psychiatry International Joint Laboratory of Henan, Zhengzhou University, Zhengzhou 450052, China. ¹³Department of Biotechnology and Biomedicine, Technical University of Denmark, DK-2800 Kgs, Lyngby, Denmark. ¹⁴Qingdao-Europe Advanced Institute for Life Sciences, Qingdao, Shandong 266555, China. ¹⁵Laboratory of Genomics and Molecular Biomedicine, Department of Biology, University of Copenhagen, DK-2100 København, Denmark. ¹⁶Department of Neurobiology, NHC and CAMS Key Laboratory of Medical Neurobiology, School of Brain Science and Brain Medicine, and MOE Frontier Science Center for Brain Science and Brain-machine Integration, Zhejiang University School of Medicine, Hangzhou 310058, China. ¹⁷These authors contributed equally: Zhiming Li, Jianbo Lai, Peifen Zhang and Jiahong Ding. ✉email: sbp@bio.dtu.dk; kk@bio.ku.dk; fccsongxq@zju.edu.cn; niechao@genomics.cn; dorhushaohua@zju.edu.cn

Received: 12 October 2021 Revised: 6 April 2022 Accepted: 7 April 2022

Published online: 20 April 2022

production of short-chain fatty acids (SCFAs) [6, 10, 11], and associated with glutamate and gamma-aminobutyric acid (GABA) metabolism [9]. However, due to the limited number of studies, modest sample sizes and inconsistent methodology, more investigations with updated databases and high-resolution metagenomic sequencing technologies are essential to uncover the interrelationship between altered gut microbiota and BD aetiology [10–12].

Beyond the mere identification of BD-related microbial taxa, attempts have been made to interpret the potential functionality of 'signature' gut microbes. One important aspect was to examine the gut microbiota-derived metabolites. In fact, there had been a growing interest in investigating the role of microbial tryptophan-kynurenine metabolism pathway in BD aetiology [13, 14]. The reason may be that not only is tryptophan the precursor of serotonin, a neurotransmitter is well known for its entangled relationship with mood disorders [15]; but also altered levels of tryptophan, kynurenine, kynurenic acid and xanthurenic acid were found in the metabolic profiling of BD, defined as dysregulated kynurenine pathway [13]. Notably, the bloodstream, a transporter of metabolites, acted as a bridge for the 'crosstalk' between the brain and the gut microbiota [7]. Studies had shown that the serum metabolome of BD patients differed from that of healthy individuals, reflecting changes in pathways related to the metabolism of specific amino acid, lipid, the citric acid cycle and polyunsaturated fatty acids [16–18]. However, serum metabolomic alterations could be disease-specific or associated with medications to treat BD [17–19]. Therefore, a cross-sectional design with drug-naïve or drug-free patients would be desirable to detect the metabolic biomarkers for BD.

In an attempt to fully explore the components of the MGB axis and how the gut microbiota may influence host metabolism and neural networks, we hypothesised that an integrated analysis of the gut microbiota, the serum metabolome and resting-state functional connectivity (rsFC) might not only unravel their relationships but also reflect the pathophysiological underpinnings of BD.

From a multi-omics approach, we employed shotgun metagenomic sequencing, untargeted mass spectrometry, and resting-state functional magnetic resonance imaging (rs-fMRI) to investigate the multidimensional differences between 109 unmedicated, depressed BD patients and 40 healthy counterparts. With the advantage of high-resolution technologies and multidimensional data, we would be in a better position to identify quantifiable and informative biomarkers for BD. Moreover, plausible interactive links between the gut and the brain could be evaluated through the concomitant changes between different omics. The current study would help to provide a comprehensive landscape of the gut-brain axis in the clinical context of acute bipolar depression.

METHODS

Ethics statement

As part of the Integrated Study of Bipolar Disorder (ISBD, ChiCTR-COC-17011401), this study was approved by the Ethics Committee of the First Affiliated Hospital, School of Medicine, Zhejiang University (Ref.2017-397) and the BGI Review Board of Bioethics and Biosafety (BGI-IRB20153). All applicable institutional regulations concerning the ethical use of information and samples from human participants were followed during this study. Each individual or his/her legal guardian provided the signed informed consent before enrolment.

Human population recruitment

A hundred and nine BD patients with a current depressive episode and forty healthy controls from the same geographical area (Zhejiang Province, China) were recruited from the Department of Psychiatry, the First Affiliated Hospital, Zhejiang University School of Medicine. According to the Diagnostic and Statistical Manual of Mental Disorders, 4th Edition (DSM-IV) criteria for BD-I, BD-II and BD not otherwise specified (NOS), the diagnosis was confirmed by two trained psychiatrists fulfilling the Chinese version of the Mini-International Neuropsychiatric Interview (MINI) through

a structured clinical interview. The 24-item Hamilton Depression Rating Scale (HAM-D-24) [20] and the Montgomery–Åsberg Depression Rating Scale (MADRS) [21] were used to evaluate the severity of depression; the Hamilton Anxiety Rating Scale (HAMA) [22] was used to measure the severity of anxiety; the Young Mania Rating Scale (YMRS) [23] was used to assess the severity of mania. The HAM-D-24 score ≥ 14 was defined as 'having a current depressive episode' and was set as the threshold for inclusion. All patients needed to meet the following inclusion criteria: (i) HAM-D-24 score no less than 14; (ii) drug-naïve or drug-free for at least 3 months; (iii) no other psychiatric comorbidity or apparent suicidal thoughts (suicidal ideation scored ≤ 2 in MADRS) to exclude individuals not suitable for standardised pharmacotherapy in the ISBD study. Exclusion criteria included: (i) chronic, severe cardiovascular or cerebrovascular diseases or other organic diseases of the brain (e.g. epilepsy and tumours); (ii) chronic or acute inflammatory, autoimmune disorders; (iii) history of substance abuse, such as alcohol and tobacco; (iv) current pregnancy or breastfeeding subjects; (v) consumption of antibiotics, prebiotics or probiotics within 4 weeks before screening; (vi) having contraindications for MRI scanning (e.g. metal implant); (vii) failing to provide the informed consent. HCs with no DSM-IV psychiatric disorders were recruited from local communities and were required to abide by the exclusion criteria. Laboratory examinations on the thyroid function, blood inflammatory factors and T-cell subsets in patients were performed to identify potential physical illnesses. Prior to the enrolment, all the participants were inquired about their dietary habits to exclude individuals with special dietary requirements, such as food allergy, food intolerance, vegetarianism, or due to religious or cultural reasons. Other relevant demographic and clinical profiles e.g. age, sex, height, weight, body mass index (BMI), marital status, drinking and smoking history, age of onset and previous history of medication of participants were collected (Supplementary Table 1). Notably, there was no significant difference between the BD group and the HC group in relation to age, sex, and BMI, analysed by Wilcoxon's rank-sum test and Fisher's exact test ($p > 0.05$; Supplementary Table 2).

Stool and plasma sample collection

Faecal samples from all 149 recruited participants were collected during the clinical examination visit. Participants were asked to deposit stool into a collection bowl and hand the bowl over to a clinical assistant. The stool sample was aliquoted using a scoop into a tube which was snap-frozen in dry ice and stored at -80°C within half an hour after collection. A blank swab was added to the faecal preservation solution as a control. The elbow vein blood (5 ml) was collected from 80 BD patients and 38 HCs (thirty-one individuals out of the total 149 participants refused to be sampled, and were thus removed from this session) during 6 a.m. to 7 a.m. in a fasting state with vacutainer tubes containing heparin, and was immediately centrifuged for 10 min (3000 rpm, 4°C). Each aliquot (1.5 ml) of the plasma samples was stored at -80°C until the ultrahigh-performance liquid chromatography was performed with liquid chromatography-mass spectrometry (LC/MS) analysis.

Metabolome profiling of human serum samples

Sample preparations. Untargeted metabolomics analysis using LC/MS was conducted. Briefly, the supernatant of the NIST standard curve correction solution was obtained by mixing the serum sample with 80% methanol, vortexed, and centrifuged at 12,000 rpm at 4°C for 10 min. After thawing all samples at 4°C , the samples for quality control and LC-MS detection were prepared at the same centrifuge condition as previously described [24].

LC-MS-based serum metabolic profiling and identification of metabolites. The raw data was converted into the mzXML format using ProteoWizard (v3.0.8789). The identification, filtration and alignment of peaks were conducted by the R-package XCMS (R-v3.1.3). After quality control, the metabolite annotations of the LC-MS data were verified using databases including LipidMaps (<http://www.lipidmaps.org>), massbank (<http://www.massbank.jp/>), Human Metabolome Database (HMDB) (<http://www.hmdb.ca>), Metlin (<http://metlin.scripps.edu>), mzcloud (<https://www.mzcloud.org>), as well as the metabolome database, which was constructed by the BioNovoGene (Suzhou, China) to avoid missing any important metabolite.

Metabolite pathway identification

The biological pathways of key metabolites that manifested significant differences between BD patients and HCs were annotated. Biological pathway analysis was performed through metabolite set enrichment analysis using the MetaboAnalyst tool suite [25].

MRI data acquisition and processing

Acquisition. Forty-four BD patients and thirty-seven HCs (68 individuals out of the total 149 participants were not able to attend the MRI session) underwent a 20-min MRI session including structural and functional scans on a 3.0 Tesla GE Signa HDxt scanner (GE Healthcare, Waukesha, Wisconsin, USA), equipped with an eight-channel phased array head coil. All subjects were instructed to remain still and awake with their eyes open during the whole session. Cushions were used to restrict head movements and earplugs for reducing the noise.

Resting-state functional images using an echo-planar imaging protocol were acquired with the following parameters: TR (repetition time) = 1800 ms, TE (echo time) = 30 ms, flip angle = 90 degrees, voxel size = $3.75 \times 3.75 \times 4 \text{ mm}^3$, field of view = $240 \times 240 \text{ mm}^2$, 28 axial slices per volume, 180 time points/volumes. High-resolution 3D T1-weighted magnetisation-prepared rapid acquisition with gradient echo (MPRAGE) structural images were acquired for anatomical reference, with parameters of TR = 7.05 ms, TE = 2.85 ms, flip angle = 8 degrees, voxel size = 1 mm^3 isotropic, field of view = $240 \times 240 \text{ mm}^2$.

Data preprocessing and denoising. Both structural and functional images were preprocessed with the CONN-20.b toolbox [26] (<http://www.nitrc.org/projects/conn>, default preprocessing pipeline), based on SPM12 [27]. Functional scans were realigned to the corresponding T1 images and resampled along the phase-encoded direction to carry out susceptibility distortion correction for adjusting head motion and possible deformation due to field inhomogeneities (realign and warp). Functional slices (interleaved and bottom-up) were time-shifted and resampled for slice-timing correction. Since functional images were notoriously prone to head motion artefacts, a more conservative approach to detecting outlier scans due to excessive head motion was employed. Scans with composite subject motion threshold over 0.5 mm or the observed global blood-oxygen-level-dependent (BOLD) signal changes above 3 standard deviations were marked as outliers [28].

All anatomical and functional images were normalised to the standard Montreal Neurological Institute (MNI) space, and then segmented into grey matter, white matter, and cerebrospinal fluid (CSF) classes (segmentation and normalisation). Direct normalisation mapped the functional data (interpolated in isotropic 2 mm voxels; resolution consistent with the MNI average mask) to the reference structural data. The resulting functional data were smoothed with a Gaussian kernel of 6 mm full-width half maximum to boost the BOLD signal-to-noise ratio. To further mitigate the influence of motion-related and physiological noise, necessary denoising procedures had been applied. CONN's anatomical component correction strategy computed the confounding effects of noise components from white matter and CSF, which were linearly regressed out of the global signal using aCompCor [29]. Band-pass filtering [0.008 Hz, 0.09 Hz] was employed to the preprocessed functional time series.

Regions of interest (ROIs). We defined the whole brain (excluding the cerebellum) into 136 different ROIs to conduct the ROI-based rsFC analysis. Ninety-one bilateral cortical ROIs were defined from FSL Harvard-Oxford Atlas maximum likelihood cortical atlas [30] and fifteen bilateral subcortical ROIs were defined from FSL Harvard-Oxford Atlas maximum likelihood subcortical atlas (see Supplementary Table 9 for the ROIs list). Based on CONN's default clustering and ordering algorithms, we also included an additional 30 networks-based ROIs defined from CONN's independent component analysis of the Human Connectome Project dataset [26] into the rsFC analysis.

Neuroimaging analyses. We investigated the ROI-based rsFC at the subject level with the CONN-20.b toolbox [31]. Average BOLD timeseries of all predefined ROIs were analysed in a pairwise manner to compute the Fisher-transformed bivariate correlation coefficient between each pair of ROIs. Pairwise ROI-to-ROI connectivity (RRC) matrix characterised the entire networks of connections for each subject. Subject-level RRC matrices were extracted from CONN to be studied subsequently with serum metabolome and gut microbiome data.

We examined between-sample RRC matrices (BD vs HC group) and carried out the functional network connectivity analysis using multivariate parametric generalised linear models (GLM) [32], where group-relevant functional connections were organised into significant network clusters with a cluster-level false discovery rate (FDR)-corrected $p < 0.05$ threshold.

Faecal DNA extraction and metagenomic sequencing

According to the manufacturer's instructions, DNA was extracted from thawed faecal samples with OMEGA-soil DNA Kit (Omega Bio-Tek, USA). The extracts were treated with DNase-free RNase to eliminate RNA contamination. The DNA quality was examined by NanoDrop 2000 UV-vis spectrophotometer and 1% agarose gel electrophoresis. The DNA library was constructed according to the manufacturer's instructions (Illumina). Applying the same workflow as described previously [33], we constructed one paired-end (PE) library with an insert size of 350 bp for each sample, followed by a high-throughput sequencing with PE reads of length 2×150 bp, using NEXTFLEX Rapid DNA-Seq (BioScientific, Austin, TX, USA). PE sequencing was performed on Illumina NovaSeq (Illumina Inc., San Diego, CA, USA). Low quality or human genomic DNA reads were removed [34]. Human genomic DNA reads were identified via SOAP2.21 [35] and were removed if they shared >95% sequence [34] with the human genome reference sequence (hg38).

Construction of species and KO profiles

The high-quality reads were aligned to the gut microbiome genomes catalogue [36] by bwa (default parameters) and $91.97 \pm 3.31\%$ reads ($n = 149$; Supplementary Table 4) were mapped. Sequence-based contigs abundance profiling was performed [37] by `jgi_summarize_bam_contig_depths` (default parameters). Reads were mapped to the genomes catalogue and the number of reads counted formed a mapping depth or abundance matrix. Considering the different sequencing depths of different samples, we used the mapping depth matrix of normalisation to estimate the abundances of contigs. For the species profile, we used the species assignment of each contig from the original genome catalogue and took the median of the relative abundance of contigs from the same species to generate the abundance of that certain species. The KO functional profile of each species was estimated as follows: the relative abundance of a KO was calculated as the summation of the relative abundance of its corresponding contigs.

Species count, α -diversity and β -diversity

The calculation of species count was based on a documented method [38], which was to tally non-zero species in each sample. The α -diversity (within-sample diversity) was estimated on the basis of the gene profile of each sample according to the Shannon index, using R (3.5.0) `vegan` package [39]. The `vegdist` function in `vegan` package was implemented to compute the Bray-Curtis dissimilarity and the β -diversity (between-sample diversity).

Statistical analysis

Multivariate analysis. Multivariate statistical analyses were applied to discriminate between BD patients and healthy individuals. Principle component analysis (PCA) of subject-level RRC matrices was performed, using the `ade4` package in the R platform [40]. Distance-based redundancy analysis (dbRDA) was carried out based on the Bray-Curtis dissimilarity on the serum metabolome, gut microbial composition and functional profile using `capscale` [39] (function of the `vegan` package in R).

Co-inertia analysis (CIA) analysis. CIA was performed on gut microbial abundance profiles and brain functional RRC matrices profiles, serum metabolite abundance profiles and functional RRC matrices of samples to assess the relationship between gut microbiome, serum metabolome and rsFC.

PERMANOVA tests. PERMANOVA [41] was conducted on the species-abundance and serum metabolite profiles of the samples to assess the effect of each clinical measure [42] using the Bray-Curtis dissimilarity and 999 permutations in R (3.5.0, `vegan` package [39]). Clinical measures with adjusted $p < 0.05$ were considered salient to associate with species and serum metabolites. In addition, we applied the PERMANOVA to investigate the possible effects of each BD-related serum metabolites and gut species on the significant rsFC clusters in bipolar brains. Gut species and serum metabolites with adjusted $p < 0.05$ were considered salient to associate with the alterations of rsFC in BD.

Association analysis. Spearman's correlation was used to ascertain the pairwise correlations between clinical measures, BD-related serum metabolites, BD-related gut microbial function and BD-related gut microbial composition [43].

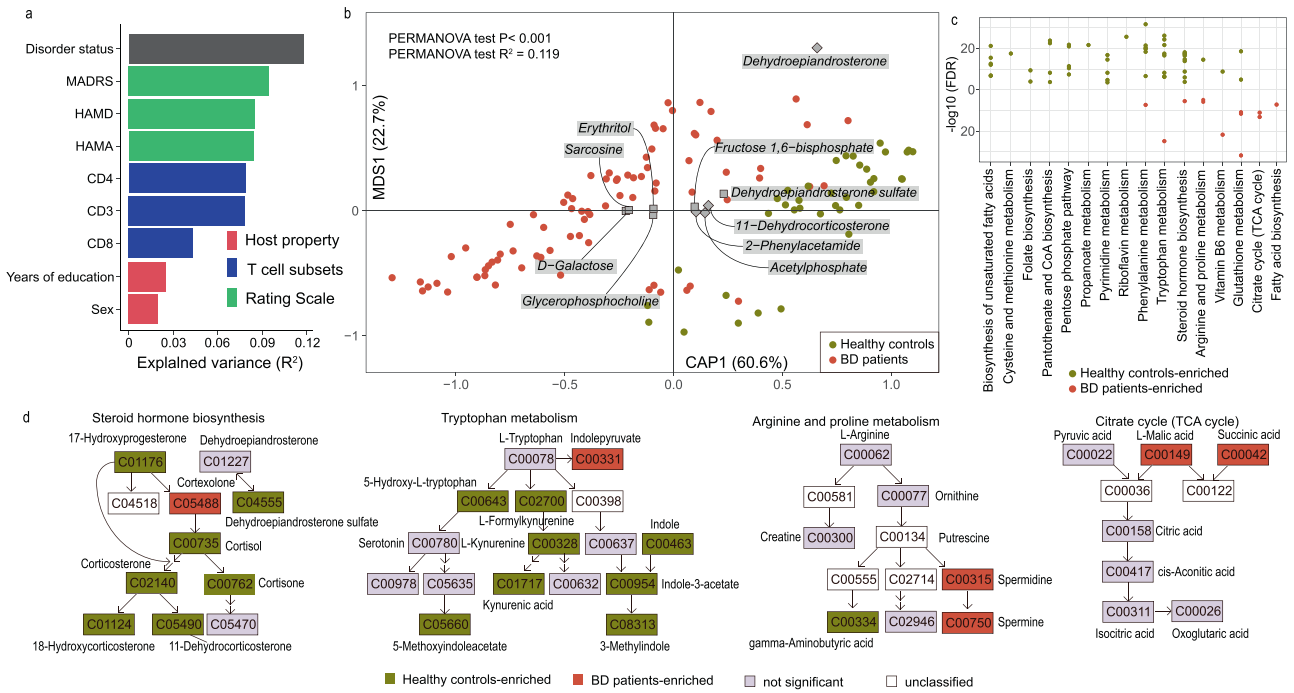


Fig. 1 Altered metabolites in serum of BD patients compared to healthy controls. **a** The effect size of phenotype indices contributed significantly to the variance (R^2) of the serum metabolome (all subjects, BD: 80, HC: 38). **b** A clear discrepancy of serum metabolomes between BD patients and healthy controls, revealed by the dbrDA. The metabolites (squares), which were identified as the main contributors to the discrepancy are specified. **c** Major metabolic pathways involved in the differentially enriched metabolites comparing BD patients and healthy controls. **d** Reaction steps for steroid hormone biosynthesis, tryptophan metabolism, arginine and proline metabolism, and citrate cycle (TCA cycle). Metabolites enriched in HCs are shown in yellow, whereas the metabolites enriched in the BD are shown in red.

Hypothesis testing and multiple testing correction. Differential abundance of gut microbial composition, gut microbial function and serum metabolites were tested by two-tailed Wilcoxon's rank-sum test between HCs and BD patients. Functional connectivity strength of rs-fMRI was tested by Analysis of Variance (ANOVA) between HCs and BD patients. FDR adjustment was employed by the Benjamin-Hochberg method [44] (using the R package *p.adjust*), and the local FDR was provided in the article.

Random forest models

According to the previously reported method [45], the concentrations of neuroactive metabolites in serum and disorder status classification were modelled using the random forest 4.6–12 package [46] based on the species' compositional profiles.

Variable selection. Firstly, the random forest regression model was used to predict the concentration of the serum metabolites, and the largest variable of IncMSE was selected as the first variable. Secondly, the first variable and the remaining variables were combined into two variables to predict the neuroactive metabolites, and the Q^2 values of the predicted results were computed and compared (the variables that maximise Q^2 were selected). More variables were added iteratively in the same way, until Q^2 was no longer increased.

$$Q^2 = 1 - \frac{\sum (y_i - \hat{y}_i)^2}{\sum (y_i - \bar{y})^2}$$

y_i and \hat{y}_i are the i -th observation value and predicted value of the serum metabolites, respectively.

Model training. Neuroactive metabolites were predicted by the variables selected above, where Q^2 was calculated, and the variables of importance were obtained.

Cross-validation. We applied the leave-one-out cross-validation method. Each sample was independently assumed as a validation set, and the remaining 117 samples were assumed as training sets. Q^2 was calculated by the predicted value and the experimental value. Cross-validation was used throughout all random forest modelling processes.

RESULTS

Serum metabolomic profiling reveals an apparent disparity between BD patients and HCs

Serum samples were analysed by untargeted LC/MS. After quality control, data filtering, and normalisation (see Methods), we identified 12,127 metabolic features across 118 samples. Of these, 8918 features (73.54%) were altered in BD (FDR < 0.05), indicating extensive metabolic changes in BD patients. To investigate the potential function of BD-related metabolites, we first annotated metabolic features by using the Kyoto Encyclopedia of Genes and Genomes (KEGG) database. A total of 265 annotated serum metabolites were obtained, including plasma metabolites with important functions in humans. Given the symptomatologic complexity and heterogeneity of BD, we also collected behavioural data from patients, including diagnostic questionnaires and demographic information (Supplementary Table 1). Notably, we found no evidence that behavioural measures were directly related to the serum metabolome (PERMANOVA test, $p > 0.05$). Nevertheless, the severity of BD symptoms (quantitative measures derived from questionnaires of MADRS, HAMD and HAMA) and the proportion of T-cell subsets were significantly associated with the serum metabolome (Fig. 1a, PERMANOVA test, $p < 0.01$). Additionally, we found that years of education and sex exerted moderate but statistically significant effects on the serum metabolome of patients with BD (Fig. 1a, PERMANOVA test, $p < 0.05$). The BD disease status, which accounted for almost 12% of the variance, was the main factor for changes in the serum metabolome, distinguishing BD patients from HCs (Fig. 1a).

We further examined the data with a dbrDA and found that the serum metabolome in BD patients was in stark contrast to that of HCs (Fig. 1b PERMANOVA test, $p < 0.01$), where 138 of 265 metabolites were significantly associated with BD (Supplementary Fig. 1 and Supplementary Table 3). Moreover, we observed that levels of more than half (73.2%) of the metabolites were reduced across all BD patients (FDR < 0.05, |fold change| > 1.35;

Supplementary Fig. 1 and Supplementary Table 3). The BD patients exhibited distinct patterns of metabolic pathway changes, where the 138 serum metabolites were involved in 64 metabolic pathways, including citrate cycle, fatty acid biosynthesis, glutathione metabolism and arginine and proline metabolism (Fig. 1c, d and Supplementary Table 3). Metabolites that were reduced in abundance in BD reflected pathways involved in steroid hormone biosynthesis, tryptophan metabolism, phenylalanine metabolism, pyrimidine metabolism, pantothenate and CoA biosynthesis, and butanoate metabolism (Supplementary Table 3). Similarly, we found that the decrease of serum GABA, common in BD patients, might be pertinent to the increase of spermine as they shared the same precursor, putrescine (Fig. 1d). The concomitant co-variation of GABA and neuroactive steroids in BD, found in the present study, demonstrated the theoretical plausibility of targeting neuroactive steroids in future BD treatment (Fig. 1d).

Mounting evidence further suggested that dysregulation of the metabolic fate of tryptophan via the kynurenine pathway may be implicated in a range of severe psychiatric disorders, including BD [47, 48]. In line with previous studies [49], the levels of kynurenine and kynurenic acid were significantly lower in BD patients than those in HCs (Fig. 1d). Notably, we found that indolepyruvate, enriched in BD patients, might compete with the synthesis of kynurenic acid and serotonin, all of which shared the same precursor, tryptophan (Fig. 1d). Additionally, vitamins involved in the production of neurotransmitters were significantly correlated with the symptom severity of BD, including folic acid (vitamin B9), pyridoxine (vitamin B6), pantothenic acid (vitamin B5) and riboflavin (vitamin B2) (Supplementary Fig. 2), suggesting the potential effects of regulating vitamin intake on BD symptoms. Essential amino acids [50] and vitamins [51] cannot be synthesised by humans and have to be acquired from the diet. In addition, tryptophan derivatives (kynurenine, kynurenic acid, serotonin), tyrosine derivatives (tyramine, dopamine), and some B-vitamins (such as folic acid, pantothenic acid and pyridoxine) have been reported to be produced by the gut microbiota via the degradation of diet-derived amino acids and purine [52, 53] (Supplementary Fig. 3).

We clustered BD-related serum metabolites (Supplementary Table 3) and examined associations of cluster abundance with the symptom severity in BD patients. Importantly, the clusters including “neuroactive metabolites” of gut microbiota derivatives (B-vitamins, kynurenic acid, GABA, SCFA derivatives) were strongly associated with the symptom severity of BD across the entire cohort (Supplementary Fig. 4). Taken together, we here discovered apparent changes in serum metabolomics of BD; results that in part could be explained through the analysis of metabolic pathways.

Taxonomic and functional characterisation of the gut microbiota in BD

To investigate whether the gut microbiota-mediated metabolomic changes in BD, we analysed the gut microbiota using metagenome shotgun sequencing across the 149 faecal samples, generating an average of 107.3 million high-quality reads (16.1 Gb of data) per sample on an Illumina HiSeq platform (Supplementary Table 4). The high-quality sequencing reads were aligned to a comprehensive reference, Unified Human Gastrointestinal Genome (UHGG), comprising 4644 species-level genomes [36], which allowed on average $91.9 \pm 0.03\%$ of the reads to be mapped (Supplementary Table 4), highlighting a considerable coverage of the gut microbiome for subsequent analyses. The classification resulted in a total of 3835 inferred prokaryotic species, and annotation of 9106 functional categories using the KEGG database.

With respect to the behavioural data, we found that the BD disease status was the major factor contributing to the alterations in the gut microbiome. The severity of BD symptoms was also

significantly associated with microbial changes. In addition, BMI and sex were associated with the gut microbiome changes in BD patients (PERMANOVA test, $p < 0.05$, Supplementary Fig. 5a). BD patients had significantly lower species counts ($p < 0.01$) and bacterial Shannon-diversity ($p = 0.062$) than controls (Supplementary Fig. 5b, c), indicating that the diversity and richness of the gut microbiota in BD patients were relatively poor. We observed a higher β diversity of the BD microbiota ($p < 0.01$), implying a more heterogeneous community structure among BD individuals than that in HCs (Supplementary Fig. 5e). The dbRDA showed that the taxonomic composition and functional potential of the BD microbiota differed markedly from that in HCs (Supplementary Fig. 5e, f), where we identified 600 species associated with BD (Fig. 2a and Supplementary Table 5, FDR < 0.05 , $|\text{fold change}| > 2$). Specifically, 136 species were enriched in BD patients, while 464 were depleted (Fig. 2a and Supplementary Table 5); species that were most enriched in BD patients included *Streptococcaceae* (nine species; *Streptococcus mitis*, *Streptococcus oralis*, *Streptococcus pseudopneumoniae*, *Streptococcus mitis* and *Streptococcus spp.*), *Fusobacteriaceae* (three species; *Fusobacterium varium* and *Fusobacterium spp.*), *Tissierellaceae* (one species; *Urmittella timonensis*), *Bacteroidaceae* (three species; *Bacteroides barnesiae*, *Bacteroides togonis* and *Bacteroidaceae spp.*), and *Actinomycetaceae* (five species; *Actinomyces graevenitzii*, *Actinomyces oris*, *Actinomyces spp.* and *Varibaculum cambriense*) (Fig. 2a and Supplementary Table 5). Depleted species included *Akkermansia* (four species; *Akkermansia muciniphila* and *Akkermansia spp.*), *Yersiniaceae* (five species; *Yersinia aleksiciae*, *Yersinia frederiksenii* and *Serratia spp.*), *Enterobacteriaceae* (12 species; *Citrobacter freundii*, *Citrobacter werkmanii*, *Citrobacter spp.*, *Cronobacter malonaticus*, *Enterobacter cancerogenus*, *Enterobacter cloacae*, *Enterobacter kobei* and *Enterobacter mori*), *Acidaminococcaceae* (eight species; *Acidaminococcus fermentans*, *Acidaminococcus spp.*, *Phascolarctobacterium succinatutens* and *Phascolarctobacterium spp.*), *Eubacteriaceae* (13 species; *Eubacterium eligens*, *Eubacterium spp.*), *Ruminococcaceae* (43 species, *Ruminococcaceae spp.*, *Ruminococcus spp.*, *Faecalibacterium prausnitzii*, *Anaerotruncus colihominis* and *Anaeromas silibacillus*), *Morganellaceae* (three species, *Providencia alcalifaciens*), *Flavobacteriaceae* (two species, *Flavobacterium spp.*) (Fig. 2a, Supplementary Fig. 6 and Supplementary Table 5). With respect to the existing literature, *Streptococcaceae* is of particular interest, as several *Streptococcaceae*, including *S. vestibularis*, have been found to be associated with schizophrenia [54]. *A. muciniphila* negatively correlated with BMI (Spearman correlation, $r = -0.14$, $p = 0.0976$), which was depleted in BD patients, was also reported to be decreased in overweight, obesity, type 2 diabetes mellitus, and hypertension [55–57]. Consistent with the previous finding of *Enterobacteriaceae* (unclassified genus) related to BD [58], our analysis here identified nine species of *Enterobacteriaceae* associated with BD (Fig. 2b).

Functional analyses of single species showed that species enriched in BD/HC encoded functions related to neuroactive metabolites mediating central neuronal processes, such as acetyl-CoA metabolism, polyamine biosynthesis, cofactor and vitamin biosynthesis, and aromatic amino acid metabolism (Supplementary Fig. 7). 15.4% of the BD-enriched species and 17.3% of the HC enriched species displayed significant differences in these functions, possibly reflecting disturbances of acetyl-CoA, polyamine, aromatic amino acid, cofactor, and vitamin availability in BD. In addition, BD/HC enriched species encoded a variety of amino acid, carbohydrate, and methane metabolic functions (Supplementary Fig. 8). More importantly, these microbial-derived functions concomitantly changed with the corresponding BD-associated serum metabolites (Fig. 3). We thus concluded that the enrichment of metabolites in BD patients was associated with gut microbiota-mediated AAA biosynthesis, SCFA biosynthesis, choline-related function, cofactor and vitamin biosynthesis.



Fig. 3 Relationships between specific gut microbial functions and the concentration of BD-related serum metabolites. The heatmap displays the Spearman correlation coefficients between functional modules and serum metabolite clusters. Black boxes highlight the BD-associated metabolites and their corresponding functional modules. The significance levels in the correlation tests are denoted as: + $p < 0.05$; * $p < 0.01$; ** $p < 0.001$. Details of metabolite clusters were shown in Supplementary Table 3.

Ruminococcaceae spp., *Citrobacter spp.*, *Eubacterium spp.* and *Yersinia-ceae spp.* were significantly associated with neuroactive metabolites (Supplementary Fig. 12).

Guided by these findings, we applied random forest models to estimate the correlation between each neuroactive metabolite and the abundance of species that contained the metabolic pathway/synthetase-encoding genes of that particular neuroactive metabolite. Random forest models that maximised the power of the neuroactive metabolites concentration prediction in serum identified 154 microbial species (Fig. 4 and Supplementary Table 7). The models accounted for, on average, 22% of the variance of the target metabolite concentrations in serum, indicating that the corresponding species largely contributed to the production of neuroactive metabolites. *Y. frederiksenii*, *Y. aleksici*, *A. muciniphila*, *C. freundii*, *C. werkmanii*, *E. cloacae*, *Ruminococcaceae spp.* and *Enterobacter kobei* were the major constituents in the random forest models (Fig. 4 and Supplementary Table 7). Coherent with changes in neuroactive metabolites in BD patients, most of the species (28.2%) were more depleted in BD (Fig. 4 and Supplementary Table 7). Importantly, species linked to the production of neuroactive metabolites correlated robustly to BD symptom severity (MADRS, HAMD, HAMA and YMRS) (Supplementary Fig. 13). Based on these findings, we hypothesised that the intestinal microbiota could affect BD pathophysiology, possibly through regulating certain neuroactive metabolites.

A classification model based on the species discussed thus far provided an area under the receiver operating characteristic curve of 0.81, differentiating BD patients from HCs (Supplementary Fig. 14a). In this model, *A. muciniphila*, *C. freundii*, *E. cloacae* and *Y. frederiksenii* were the major contributors (Supplementary Fig. 14b). These findings suggest that microbes involved in the production of neuroactive metabolites may be potential diagnostic biomarkers of BD.

Resting-state functional connectivity patterns in BD

To further investigate to what extent the intestinal microbiota and neuroactive metabolites might influence brain activity, we collected rs-fMRI of 44 BD patients and 37 HCs (Supplementary Table 1). Based on the CONN's data-driven hierarchical clustering algorithm [26] of ROI-to-ROI spatial proximity and functional similarity metrics [31] (see Methods for detail), 9180 pairwise connections of 136 ROIs were classified into 210 clusters. We first performed the PCA and found that the RRC matrix of BD patients markedly differed from that of HCs (Fig. 5a, PERMANOVA test, $p < 0.05$). An FDR-corrected cluster-level q-value of 0.05 was applied to properly control the family-wise error rates and threshold of the RRC statistical map by merely including significant connectivity clusters (Supplementary Fig. 15). Sixty-nine out of 210 clusters were significant (GLM, $FDR q < 0.05$, Supplementary Table 8) with 1401 significant individual connections (post-hoc t -test, $FDR q < 0.05$, Supplementary Table 9), which resulted in 20 'networks' (Fig. 5b and Supplementary Table 10). All significant clusters were

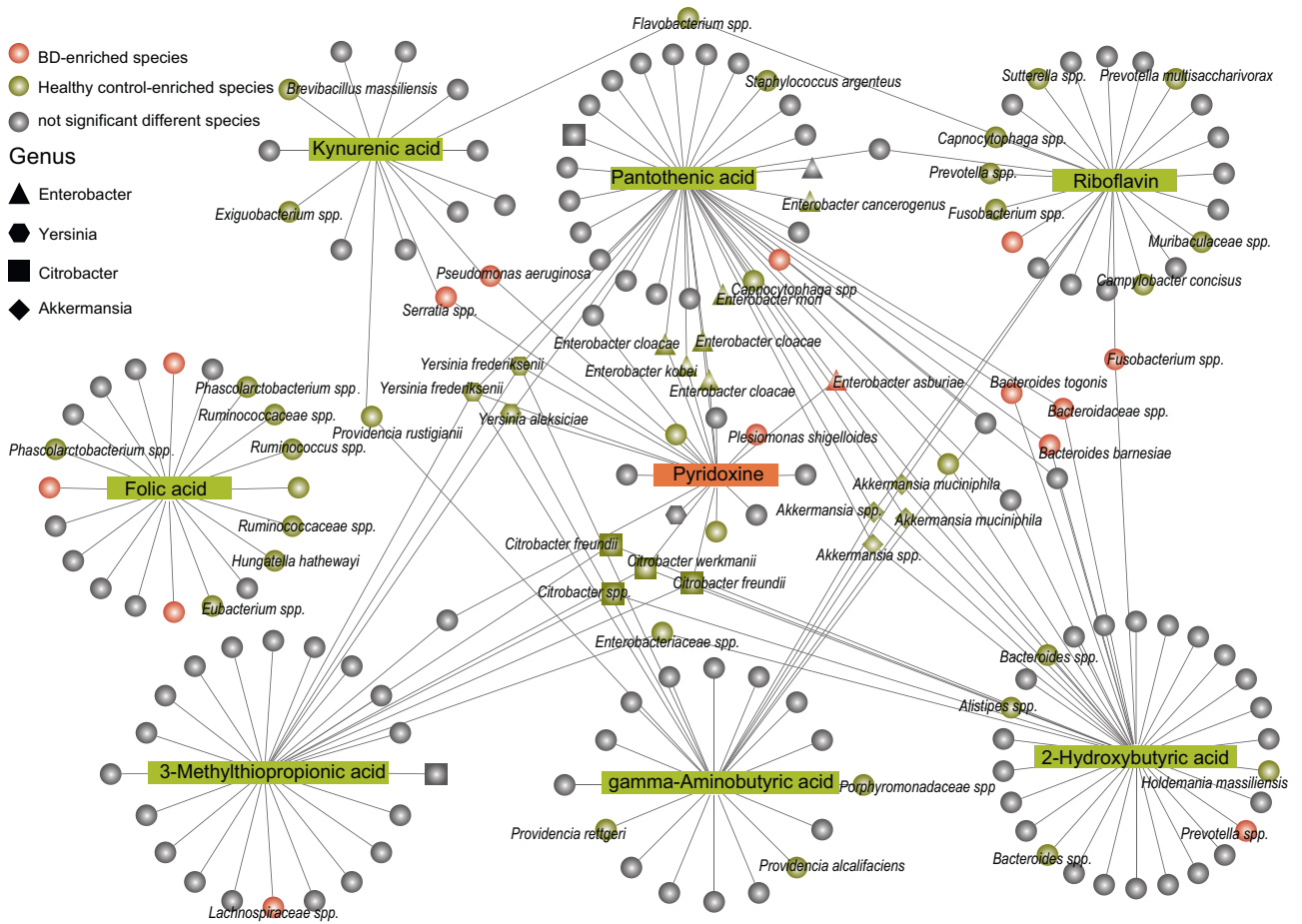


Fig. 4 Alterations in the gut microbial composition in patients with BD contribute to the loss in the biosynthesis of neuroactive metabolites. Network views of neuroactive metabolites and species. Squares represent the neuroactive metabolites and the surrounding connected circles represent the species identified in the random forest models.

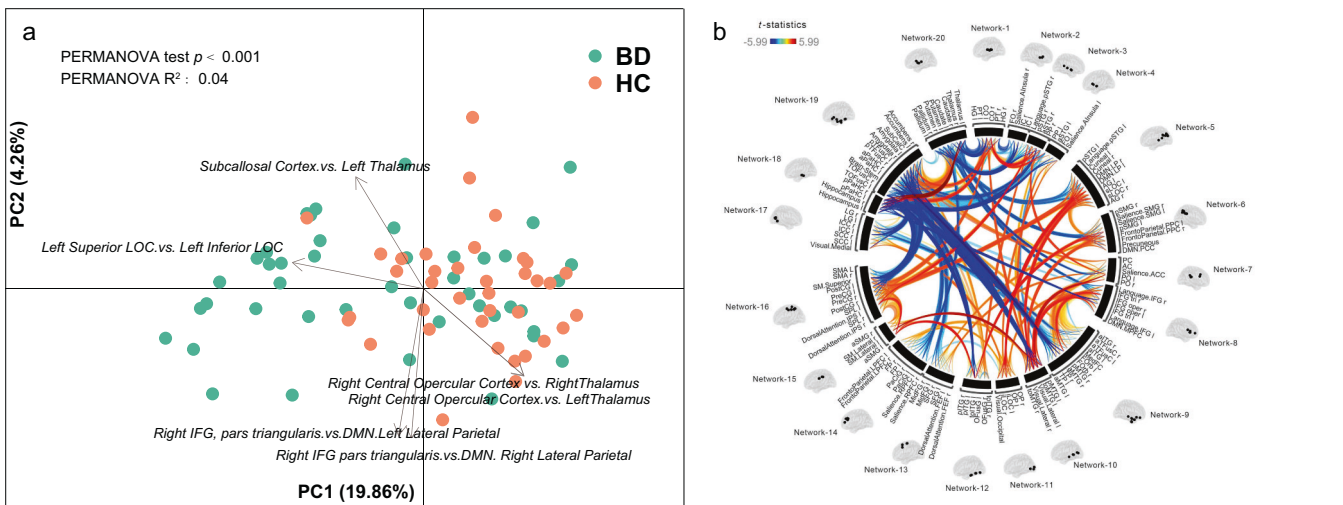


Fig. 5 Characteristics of brain functional connectivity in BD patients. **a** Differences in brain functional connectivity between patients with BD and healthy controls, was revealed by PCA. Arrows indicate the individual functional connections identified as the major contributor. **b** Functional connectome ring of BD-HC contrasts. CONN's default hierarchical clustering algorithm yielded 20 networks, displayed in sagittal brain views. All connections within- and between-networks were analyzed using GLM to establish differences in functional connectivity between BD and HC subjects. Significant clusters (FDR $q < 0.05$) with significant individual connections are shown as coloured curves (reddish scale: BD > HC contrasts; bluish scale: BD < HC contrasts). The opacity of connection curves corresponds to respective t -statistics.

between parts of the sensory regions and subcortical areas were largely attenuated in BD. The evidence seems to suggest that BD patients may experience aberrant sensory information processing and emotional appraisals of interoceptive activities [64]. Arguably, the FC patterns between the auditory areas ('network-1' and part of 'network-7') and subcortical regions were less conclusive (Supplementary Fig. 16b). Increased FC of the auditory areas with the hippocampus and amygdala and reduced FC of the auditory areas with the thalamus were both observed, which might explain the finding of some BD patients having psychosis-like experiences [65]. Converging evidence thus far has demonstrated abnormalities of FC in BD and stressed the importance of cognition, emotion, and interoceptive-sensory perception related connectivity networks.

BD-related serum metabolites and gut microbes are tightly linked to brain functional connectivity

Next, we assessed the effect size of the serum metabolomics, gut microbiota and rsFC. The effect size of the serum metabolome and rsFC (Pearson $r = 0.395$, $p = 0.039$) was greater than that of the gut microbiota and rsFC (Pearson $r = 0.368$, $p = 0.073$) (Fig. 6a, b), possibly reflecting that neural signals can alter the sensorimotor and secretory functions of the gut through complex neurohumoral pathways, and the derivatives from gut microbes can regulate the brain function through visceral and endocrine circulation afferent signals [66]. Furthermore, we analysed the association between BD-related serum metabolites/BD-related gut microbes and ROI-based FC. We found that 86.96% (120/138) of BD-related serum metabolites were significantly correlated (Supplementary Table 11, PERMANOVA test, $p < 0.05$) with at least one individual connection. In particular, folic acid, which was documented to be related to the brain development [67] and regulation of mood [68] and cognition [69], was correlated with most of the significant clusters (85.51%, 59/69, Fig. 6c and Supplementary Table 11), including brain regions and networks of the hippocampal formation and amygdala ('network-18' and 'network-19'), thalamus and striatum ('network-20'), language areas ('network-3', 'network-4' and 'network-5') and sensorimotor areas ('network-10' and 'network-16') (Fig. 6c and Supplementary Fig. 17). In addition, other neuroactive metabolites, such as kynurenic acid, pyridoxine, GABA and riboflavin were significantly associated with the FC of the thalamus and striatum ('network-20'), auditory areas ('network-7'), language areas ('network-3', 'network-4' and 'network-5'), dorsal-attention network ('network-12'), and hippocampal formation and amygdala ('network-18' and 'network-19'), suggesting that the identified dysregulation of the neuroactive metabolites in serum may affect specific brain functions, implicated to language, emotion and reward processing in BD (Fig. 6c, Supplementary Fig. 17 and Supplementary Table 11).

Likewise, 78.33% (470/600) of gut microbes were significantly correlated (Supplementary Table 12, PERMANOVA test, $p < 0.05$) with at least one individual connection. Specifically, microorganisms that were associated with neuroactive metabolites of serum were also related to specific connectivity networks. For instance, *Akkermansia* spp. (mostly *A. muciniphila*), *C. freundii*, *Yersinia* spp. (*Y. frederiksenii* and *Y. aleksiciae*), *Phascolarctobacterium* spp., *Flavobacterium* spp. and *Enterobacter* spp. (*E. cloacae* and *E. kobei*) were significantly associated with the FC of the language areas ('network-3' and 'network-4'), thalamus and striatum ('network-20'), sensorimotor areas ('network-10' and 'network-16'), and hippocampal formation and amygdala ('network-18' and 'network-19') (Fig. 6d, Supplementary Fig. 17 and Supplementary Table 12).

These results implied that the gut microbiota affected BD possibly by affecting the metabolism of certain neuroactive metabolites, which might, in turn, regulate the cognitive, emotional and interoceptive function of the bipolar brain.

DISCUSSION

Accumulating evidence suggests that disturbed gut microbiota may contribute to the pathophysiology of bipolar disorder, yet the underlying mechanism remains unresolved [70]. By comparing the gut microbiota, serum metabolome, and rsFC patterns between unmedicated BD patients and HCs, we found that BD was characterised by alterations in gut microbial composition, functional potential and metabolic pathways impinging on the MGB axis. The altered microbial and functional modules linked the gut microbiota with dysregulation of microbiota-derived neuroactive metabolites (pantothenic acid, riboflavin, folic acid, pyridoxine, kynurenic acid, GABA and SCFAs). Moreover, further analyses of functional connectivity in the bipolar brain complemented our investigation of the MGB axis, revealing disturbances in the hippocampus, amygdala, superior temporal gyrus and sensorimotor gyrus. Our multi-omics study has drawn tight lines between specific microbiota-derived neuroactive metabolites and highlighted neural networks, depicting a more nuanced picture of MGB communication and how that may affect human cognition and behaviour in the context of BD.

The crosstalk between the gut and the brain may take place through multifarious pathways. For instance, the gut microbiota can interact intimately with the intestinal immune system and thus affect neuroimmunity; microbial products and metabolites can signal through enteroendocrine cells and enterochromaffin cells to modulate the secretion of neuropeptides and neurotransmitters; microbiota-regulated hormones can directly interact with intrinsic enteric neurons and gut innervating vagal and spinal afferents; micronutrients of microbial products provide nutrition for the brain actively transporting across the blood-brain barrier [66, 71, 72]. Existing evidence has supported that mitochondrial dysfunction plays a crucial role in the aetiology of BD [73, 74]. The citrate cycle is imperative for the synthesis of mitochondrial ATP, and it was recently reported that abnormality in the citric acid cycle of the mitochondria might contribute to the development of BD [16].

Our work has contributed to the current evidence base by elaborating BD-specific neuroactive microbes and metabolites, involved in the abovementioned pathways of gut-brain communication. We found that BD-associated *A. muciniphila*, *Citrobacter* spp. (*C. freundii* and *C. werkmanii*), *Phascolarctobacterium* spp., *Yersinia* spp. (*Y. frederiksenii* and *Y. aleksiciae*), *Enterobacter* spp. (*E. cloacae* and *E. kobei*) and *Flavobacterium* spp. co-varied with multiple B-vitamins in serum, indicated by the significant deficiencies in folic acid (B9), riboflavin (B2) and pantothenic acid (B5), and excess in pyridoxine (B6) among unmedicated BD patients. In addition to dietary access, human gut microbial communities have been reported to synthesise vitamins, which are subsequently absorbed by the host in the large intestine [71, 75]. The B-vitamins serve as pivotal micronutrients to maintain brain function and mental health [71]. We observed that BD-related alterations in identified B-vitamins and relevant gut microbiota were associated with consistently weaker FC in 'network-18' (hippocampus), 'network-19' (amygdala) and 'network-20' (thalamus and striatum), and stronger FC in 'network-10' (inferior temporal gyrus) and 'network-16' (sensorimotor cortex) though the latter lacked clear-cut evidence (Supplementary Fig. 17). Similarly, GABA, SCFAs and kynurenic acid were also detected as key BD-related neuroactive metabolites that can be produced by *A. muciniphila*, *Citrobacter* spp. (*C. freundii* and *C. werkmanii*), *Phascolarctobacterium* spp., *Yersinia* spp. (*Y. frederiksenii* and *Y. aleksiciae*) and *Flavobacterium* spp. Abnormal levels of GABA in arginine and proline metabolism have been reported to be associated with BD [76]. Present literature indicates that neuroactive steroids acting at inhibitory GABA receptors might be candidate modulators of BD [77]. Apart from the robustly diminished FC of 'network-18' and 'network-19' in BD, alluding to the importance of the hippocampus and amygdala as neural

nodes of BD, heightened FC in the language and auditory areas (i.e. superior temporal gyrus; 'network-3' and 'network-5') was detected in the case of depleted GABA and SCFAs (i.e. 2-hydroxybutyric acid). Increased FC harbouring the sensorimotor areas ('network-12' and 'network-16') was more pronounced in the kynurenic acid-centred analysis (Supplementary Fig. 17).

Notably, this study has employed the latest gut genome catalogue [36] which is used as the reference for the gut microbiome, and our average mapped reads ratio has reached a high level of $91.9 \pm 0.03\%$. Based on this catalogue, we identified a few microorganisms exhibiting a strong correlation to BD, including *A. muciniphila*, *Citrobacter spp.* (*C. freundii* and *C. werkmanii*), *Yersinia spp.* (*Y. frederiksenii* and *Y. aleksiciae*) and *Enterobacter spp.* (*E. cloacae* and *E. kobei*). Compared with the previous 16 S RNA report [78–80], the current study had notably higher sensitivity and accuracy.

It is important to note that our study has been limited by the small sample size, imbalanced case-control ratio, the mere inclusion of depressive bipolar patients, and the lack of additional validation data. Arguably, the power calculation showed that the current sample size and case-control ratio were acceptable to achieve relatively satisfying statistical power (>0.8). Nevertheless, the results we reported in this study can be generalised to bipolar depression only, where we cannot preclude the possibility of patients with a current manic episode exhibiting distinct microbiome and metabolic profiles. Ideally, future studies with a larger sample size should include BD patients in both manic and depressive phases with a more balanced number of controls. It would also be of interest to compare the multi-omics differences with regard to the subtypes of BD if more type-I patients are to be recruited. Another issue is the non-targeted analysis of serum metabolomics, where more than 90% of the metabolites could not be identified. This has hampered the research for merely focusing on metabolites that are known to be relevant to the neuronal processes, namely the neuroactive metabolites. It is likely that some serum metabolites that we have overlooked may be crucial in the physiology of BD, which warrants further investigations.

Based on the current associative evidence, it is not possible to determine the causation of alterations in the gut microbiome or serum metabolome to the development of BD symptoms, which is a common limitation shared by studies of observational nature [81]. Although the exact mechanisms of how the gut microbiota affects the brain or vice versa are far from clear, our findings of specific microbes as the sources of neuroactive metabolites of interest have pointed to key signalling pathways and compounds involved in the interactions between the gut and the brain. Our future research will address this issue by utilising animal models and intervention studies to further narrow the gaps in our understanding of the MGB axis in higher-order human cognition and behaviour. For example, faecal transplantation of gut microbiota from drug-naïve or drug-free BD patients to germ-free mice may allow us to investigate whether the BD-associated gut microbial ecosystem could induce BD-like characteristics in mice models, an experimental practice that has been reported in schizophrenia research [82, 83]. Similarly, a well-controlled longitudinal intervention design makes it possible to follow and scrutinise the progression and changes of symptoms along with the timeseries-based assessment of gut microbiome and serum metabolome in BD patients.

The last decade has seen a rapidly growing field of microbiome research incorporating neuroimaging techniques and documenting how gut microbiota may influence brain structure and function [84]. Our new analytical protocol of studying the gut microbial ecosystem and serum metabolome in tandem with whole-brain functional networks provides insights for research exploiting the gut microbiota and neuroactive metabolites, e.g. B-vitamins, kynurenic acid, GABA and SCFAs, as informative biomarkers of diagnostic and prognostic potentials. This approach

may hold the particular promise for therapeutic intervention for more targeted clinical management in the near future.

In conclusion, our study has identified BD-associated microbes (*A. muciniphila*, *Citrobacter spp.* [*C. freundii* and *C. werkmanii*], *Phascolarctobacterium spp.*, *Yersinia spp.* [*Y. frederiksenii* and *Y. aleksiciae*], *Enterobacter spp.* [*E. cloacae* and *E. kobei*] and *Flavobacterium spp.*), neuroactive metabolites (B-vitamins, kynurenic acid, GABA and SCFAs) and functional connectivity networks (language processing, emotion regulation and interoception). We have comprehensively demonstrated interplays between the gut microbiota at the species level and serum metabolites in unmedicated BD patients and proposed new insights into the MGB axis and the relationship between the gut microbiota, host metabolism, and the dynamic bipolar brain.

DATA AVAILABILITY

Metagenomic and neuroimaging data have been deposited into the CNGB Sequence Archive (CNSA; <https://db.cngb.org/cnsa/>) [85] of China National GeneBank DataBase (CNGBdb) [86] with accession number CNP0002003. The datasets generated by this study are available from the corresponding authors upon request.

CODE AVAILABILITY

All codes used for data analysis including serum metabolome, gut microbiome and rs-fMRI are available on https://github.com/lizhiming11/BD_project.

REFERENCES

- Lynch SV, Pedersen O. The human intestinal microbiome in health and disease. *N Engl J Med.* 2016;375:2369–79.
- Michaudel C, Sokol H. The gut microbiota at the service of immunometabolism. *Cell Metab.* 2020;32:514–23.
- Wu J, Wang K, Wang X, Pang Y, Jiang C. The role of the gut microbiome and its metabolites in metabolic diseases. *Protein Cell.* 2020;12, 360–73.
- Simpson CA, Diaz-Arteche C, Eljiby D, Schwartz OS, Simmons JG, Cowan CS. The gut microbiota in anxiety and depression—A systematic review. *Clin Psychol Rev.* 2020;83;101943.
- Morais LH, Schreiber HL, Mazmanian SK. The gut microbiota–brain axis in behaviour and brain disorders. *Nat Rev Microbiol.* 2020;19:241–55.
- Lai J, Jiang J, Zhang P, Xi C, Wu L, Gao X, et al. Gut microbial clues to bipolar disorder: state-of-the-art review of current findings and future directions. *Clin Transl Med.* 2020;10:e146.
- Guest PC, Guest FL, Martins-de Souza D. Making sense of blood-based proteomics and metabolomics in psychiatric research. *Int J Neuropsychopharmacol.* 2016;19.
- Nikolova VL, Hall MR, Hall LJ, Cleare AJ, Stone JM, Young AH. perturbations in gut microbiota composition in psychiatric disorders: a review and meta-analysis. *JAMA Psychiatry.* 2021;78:1343–54.
- McGuinness A, Davis J, Dawson S, Loughman A, Collier F, O'Hely M, et al. A systematic review of gut microbiota composition in observational studies of major depressive disorder, bipolar disorder and schizophrenia. *Mol Psychiatry.* 2022;1–16.
- Sublette ME, Cheung S, Lieberman E, Hu S, Mann JJ, Uhlemann AC, et al. Bipolar disorder and the gut microbiome: a systematic review. *Bipolar Disord.* 2021;23:544–64.
- Huang T-T, Lai J-B, Du Y-L, Xu Y, Ruan L-M, Hu S-H. Current understanding of gut microbiota in mood disorders: an update of human studies. *Front Genet.* 2019;10:98.
- Rong H, Xie X-h, Zhao J, Lai W-t, Wang M-b, Xu D, et al. Similarly in depression, nuances of gut microbiota: evidences from a shotgun metagenomics sequencing study on major depressive disorder versus bipolar disorder with current major depressive episode patients. *J Psychiatr Res.* 2019;113:90–9.
- Bartoli F, Misiak B, Callovin T, Cavaleri D, Cioni RM, Crocarno C, et al. The kynurenic pathway in bipolar disorder: a meta-analysis on the peripheral blood levels of tryptophan and related metabolites. *Mol Psychiatry.* 2021;26:3419–29.
- Lai W-t, Deng W-f, Xu S-x, Zhao J, Xu D, Liu Y-h, et al. Shotgun metagenomics reveals both taxonomic and tryptophan pathway differences of gut microbiota in major depressive disorder patients. *Psychological Med.* 2021;51:90–101.
- Fakhoury M. Revisiting the serotonin hypothesis: implications for major depressive disorders. *Mol Neurobiol.* 2016;53:2778–86.
- Yoshimi N, Futamura T, Kakumoto K, Salehi AM, Sellgren CM, Holmén-Larsson J, et al. Blood metabolomics analysis identifies abnormalities in the citric acid cycle, urea cycle, and amino acid metabolism in bipolar disorder. *BBA Clin.* 2016;5:151–8.

17. Burghardt KJ, Evans SJ, Wiese KM, Ellingrod VL. An untargeted metabolomics analysis of antipsychotic use in bipolar disorder. *Clin Transl Sci.* 2015;8:432–40.
18. Sussulini A, Prando A, Maretto DA, Poppi RJ, Tasic L, Banzato CEM, et al. Metabolic profiling of human blood serum from treated patients with bipolar disorder employing 1H NMR spectroscopy and chemometrics. *Anal Chem.* 2009;81:9755–63.
19. Yang J, Yan B, Zhao B, Fan Y, He X, Yang L, et al. Assessing the causal effects of human serum metabolites on 5 major psychiatric disorders. *Schizophrenia Bull.* 2020;46:804–13.
20. Hamilton M. A rating scale for depression. *J Neurol Neurosurg Psychiatry.* 1960;23:56.
21. Müller M. Differentiating moderate and severe depression using the Montgomery–Åsberg depression rating scale (MADRS). *J Affect Disord.* 2003;77:255–60.
22. Hamilton M. The assessment of anxiety states by rating. *Br J Med Psychol.* 1959;32:50–5.
23. Young RC, Biggs JT, Ziegler VE, Meyer DA. A rating scale for mania: reliability, validity and sensitivity. *Br J Psychiatry.* 1978;133:429–35.
24. Feng Q, Li Y, Yang Y, Feng J. Urine metabolomics analysis in patients with non-moalbuminuric diabetic kidney disease. *Front Physiol.* 2020;11:578799.
25. Chong J, Soufan O, Li C, Caraus I, Li S, Bourque G, et al. MetaboAnalyst 4.0: towards more transparent and integrative metabolomics analysis. *Nucleic Acids Res.* 2018;46:W486–94.
26. Whitfield-Gabrieli S, Nieto-Castanon A. Conn: a functional connectivity toolbox for correlated and anticorrelated brain networks. *Brain Connectivity.* 2012;2:125–41.
27. Penny WD, Friston KJ, Ashburner JT, Kiebel SJ, Nichols TE. *Statistical parametric mapping: the analysis of functional brain images.* Burlington: Elsevier; 2011.
28. Whitfield-Gabrieli S, Nieto-Castanon A, Ghosh S. *Artifact detection tools (ART)* 2011;7:11.
29. Behzadi Y, Restom K, Liu J, Liu TT. A component based noise correction method (CompCor) for BOLD and perfusion based fMRI. *Neuroimage.* 2007;37:90–101.
30. Desikan RS, Ségonne F, Fischl B, Quinn BT, Dickerson BC, Blacker D, et al. An automated labeling system for subdividing the human cerebral cortex on MRI scans into gyral based regions of interest. *Neuroimage.* 2006;31:968–80.
31. Nieto-Castanon A. *Handbook of functional connectivity magnetic resonance imaging methods in CONN.* Boston: Hilbert Press; 2020.
32. Jafri MJ, Pearson GD, Stevens M, Calhoun VDJN. A method for functional network connectivity among spatially independent resting-state components in schizophrenia. *Neuroimage.* 2008;39:1666–81.
33. Yang J, Zheng P, Li Y, Wu J, Tan X, Zhou J, et al. Landscapes of bacterial and metabolic signatures and their interaction in major depressive disorders. *Sci Adv.* 2020;6:eaba8555.
34. Li Z, Xia J, Jiang L, Tan Y, An Y, Zhu X, et al. Characterization of the human skin resistome and identification of two microbiota cutotypes. *Microbiome.* 2021;9:1–18.
35. Li R, Yu C, Li Y, Lam T-W, Yiu S-M, Kristiansen K, et al. SOAP2: an improved ultrafast tool for short read alignment. *Bioinformatics.* 2009;25:1966–67.
36. Almeida A, Nayfach S, Boland M, Strozzi F, Beracochea M, Shi ZJ, et al. A unified catalog of 204,938 reference genomes from the human gut microbiome. *Nat Biotechnol.* 2021;39:105–14.
37. Kang DD, Li F, Kirton E, Thomas A, Egan R, An H, et al. MetaBAT 2: an adaptive binning algorithm for robust and efficient genome reconstruction from metagenome assemblies. *PeerJ.* 2019;7:e7359.
38. Le Chatelier E, Nielsen T, Qin J, Prifti E, Hildebrand F, Falony G, et al. Richness of human gut microbiome correlates with metabolic markers. *Nature.* 2013;500:541–6.
39. Oksanen J, Blanchet FG, Kindt R, Legendre P, Minchin PR, O'hara R, et al. *Package 'vegan'.* Community Ecol Package. 2013;2:1–295.
40. Dray S, Dufour A-B. The ade4 package: implementing the duality diagram for ecologists. *J Stat Softw.* 2007;22:1–20.
41. McArdle BH, Anderson MJJE. Fitting multivariate models to community data: a comment on distance-based redundancy analysis. *Ecology.* 2001;82:290–297.
42. Feng Q, Liang S, Jia H, Stadlmayr A, Tang L, Lan Z, et al. Gut microbiome development along the colorectal adenoma–carcinoma sequence. *Nat Commun.* 2015;6:1–13.
43. Karlsson FH, Tremaroli V, Nookaew I, Bergström G, Behre CJ, Fagerberg B, et al. Gut metagenome in European women with normal, impaired and diabetic glucose control. *Nature.* 2013;498:99–103.
44. Benjamini Y, YJotRssB Hochberg. Controlling the false discovery rate: a practical and powerful approach to multiple testing. *J R Stat Soc Ser B (Methodol).* 1995;57:289–300.
45. Wang X, Yang S, Li S, Zhao L, Hao Y, Qin J, et al. Aberrant gut microbiota alters host metabolome and impacts renal failure in humans and rodents. *Gut.* 2020;69:2131–42.
46. Breiman L. Random forests. *Mach Learn.* 2001;45:5–32.
47. Pu J, Liu Y, Zhang H, Tian L, Gui S, Yu Y, et al. An integrated meta-analysis of peripheral blood metabolites and biological functions in major depressive disorder. *Mol Psychiatry.* 2020;26:4265–76.
48. Lovelace MD, Varney B, Sundaram G, Lennon MJ, Lim CK, Jacobs K, et al. Recent evidence for an expanded role of the kynurenine pathway of tryptophan metabolism in neurological diseases. *Neuropharmacology.* 2017;112:373–88.
49. Marx W, McGuinness AJ, Rocks T, Ruusunen A, Cleminson J, Walker AJ, et al. The kynurenine pathway in major depressive disorder, bipolar disorder, and schizophrenia: a meta-analysis of 101 studies. *Molecular Psychiatry.* 2020;26:4158–78.
50. Cervenka I, Agudelo LZ, Ruas JL. Kynurenines: Tryptophan's metabolites in exercise, inflammation, and mental health. *Science.* 2017;357:eaaf9794.
51. Mora JR, Iwata M, Von, Andrian UH. Vitamin effects on the immune system: vitamins A and D take centre stage. *Nat Rev Immunol.* 2008;8:685–98.
52. Gevi F, Zolla L, Gabriele S, Persico AM. Urinary metabolomics of young Italian autistic children supports abnormal tryptophan and purine metabolism. *Mol Autism.* 2016;7:1–11.
53. Wikoff WR, Anfora AT, Liu J, Schultz PG, Lesley SA, Peters EC, et al. Metabolomics analysis reveals large effects of gut microflora on mammalian blood metabolites. *Proc Natl Acad Sci USA.* 2009;106:3698–703.
54. Zhu F, Ju Y, Wang W, Wang Q, Guo R, Ma Q, et al. Metagenome-wide association of gut microbiome features for schizophrenia. *Nat Commun.* 2020;11:1–10.
55. Liu R, Hong J, Xu X, Feng Q, Zhang D, Gu Y, et al. Gut microbiome and serum metabolome alterations in obesity and after weight-loss intervention. *Nat Med.* 2017;23:859–68.
56. Qin J, Li Y, Cai Z, Li S, Zhu J, Zhang F, et al. A metagenome-wide association study of gut microbiota in type 2 diabetes. *Nature.* 2012;490:55–60.
57. Yan Q, Gu Y, Li X, Yang W, Jia L, Chen C, et al. Alterations of the gut microbiome in hypertension. *Front Cell Infect Microbiol.* 2017;7:381.
58. Evans SJ, Bassis CM, Hein R, Assari S, Flowers SA, Kelly MB, et al. The gut microbiome composition associates with bipolar disorder and illness severity. *J Psychiatr Res.* 2017;87:23–9.
59. Osadchiy V, Martin CR, Mayer EA. The gut–brain axis and the microbiome: mechanisms and clinical implications. *Clin Gastroenterol Hepatol.* 2019;17:322–32.
60. Strandwitz P, Kim KH, Terekhova D, Liu JK, Sharma A, Levering J, et al. GABA-modulating bacteria of the human gut microbiota. *Nat Microbiol.* 2019;4:396–403.
61. Tran SM-S, Mohajeri MH. The role of gut bacterial metabolites in brain development, aging and disease. *Nutrients.* 2021;13:732.
62. Perry A, Roberts G, Mitchell PB, Breakspear M. Connectomics of bipolar disorder: a critical review, and evidence for dynamic instabilities within interoceptive networks. *Mol Psychiatry.* 2019;24:1296–318.
63. Altinay MI, Hulvershorn LA, Karne H, Beall EB, Anand A. Differential resting-state functional connectivity of striatal subregions in bipolar depression and hypomania. *Brain Connectivity.* 2016;6:255–65.
64. Stoddard J, Gotts S, Brotman M, Lever S, Hsu D, Zarate C Jr, et al. Aberrant intrinsic functional connectivity within and between corticostriatal and temporal–parietal networks in adults and youth with bipolar disorder. *Psychological Med.* 2016;46:1509.
65. Skåtun KC, Kauffmann T, Brandt CL, Doan NT, Alnæs D, Tønnesen S, et al. Thalamocortical functional connectivity in schizophrenia and bipolar disorder. *Brain Imaging Behav.* 2018;12:640–52.
66. Dalile B, Van Oudenhove L, Vervliet B, Verbeke K. The role of short-chain fatty acids in microbiota–gut–brain communication. *Nat Rev Gastroenterol Hepatol.* 2019;16:461–78.
67. Liu L, Liu Z, Li Y, Sun C. Integration of metabolomics and proteomics to highlight altered neural development related pathways in the adult offspring after maternal folic acid supplement. *Clin Nutr.* 2021;40:476–87.
68. Gao L, Liu X, Yu L, Wu J, Xu M, Liu Y. Folic acid exerts antidepressant effects by upregulating brain-derived neurotrophic factor and glutamate receptor 1 expression in brain. *Neuroreport.* 2017;28:1078–84.
69. Enderami A, Zarghami M, Darvishi-Khezri H. The effects and potential mechanisms of folic acid on cognitive function: a comprehensive review. *Neurological Sci.* 2018;39:1667–75.
70. Valles-Colomer M, Falony G, Darzi Y, Tigchelaar EF, Wang J, Tito RY, et al. The neuroactive potential of the human gut microbiota in quality of life and depression. *Nat Microbiol.* 2019;4:623–32.
71. Kennedy DO. B vitamins and the brain: mechanisms, dose and efficacy—a review. *Nutrients.* 2016;8:68.
72. Agirman G, Hsiao EY. SnapShot: the microbiota-gut-brain axis. *Cell.* 2021;184:2524.
73. Goldstein BI, Young LT. Toward clinically applicable biomarkers in bipolar disorder: focus on BDNF, inflammatory markers, and endothelial function. *Curr Psychiatry Rep.* 2013;15:425.
74. de Sousa RT, Machado-Vieira R, Zarate CA Jr, Manji HK. Targeting mitochondrially mediated plasticity to develop improved therapeutics for bipolar disorder. *Expert Opin Therapeutic Targets.* 2014;18:1131–47.
75. Das P, Babaei P, Nielsen J. Metagenomic analysis of microbe-mediated vitamin metabolism in the human gut microbiome. *BMC Genomics.* 2019;20:1–11.

76. Brady RO Jr, McCarthy JM, Prescott AP, Jensen JE, Cooper AJ, Cohen BM, et al. Brain gamma-aminobutyric acid (GABA) abnormalities in bipolar disorder. *Bipolar Disord.* 2013;15:434–9.
77. Marx CE, Stevens RD, Shampine LJ, Uzunova V, Trost WT, Butterfield MI, et al. Neuroactive steroids are altered in schizophrenia and bipolar disorder: relevance to pathophysiology and therapeutics. *Neuropsychopharmacology.* 2006;31:1249–63.
78. Zheng P, Yang J, Li Y, Wu J, Liang W, Yin B, et al. Gut microbial signatures can discriminate unipolar from bipolar depression. *Adv Sci.* 2020;7:1902862.
79. Rhee SJ, Kim H, Lee Y, Lee HJ, Park CHK, Yang J, et al. Comparison of serum microbiome composition in bipolar and major depressive disorders. *J Psychiatr Res.* 2020;123:31–8.
80. McIntyre RS, Subramaniapillai M, Shekotikhina M, Carmona NE, Lee Y, Mansur RB, et al. Characterizing the gut microbiota in adults with bipolar disorder: a pilot study. *Nutr Neurosci.* 2021;24:173–80.
81. Wang DD, Nguyen LH, Li Y, Yan Y, Ma W, Rinott E, et al. The gut microbiome modulates the protective association between a Mediterranean diet and cardiometabolic disease risk. *Nat Med.* 2021;27:333–43.
82. Zheng P, Zeng B, Liu M, Chen J, Pan J, Han Y, et al. The gut microbiome from patients with schizophrenia modulates the glutamate-glutamine-GABA cycle and schizophrenia-relevant behaviors in mice. *Sci Adv.* 2019;5:eaau8317.
83. Zhu F, Guo R, Wang W, Ju Y, Wang Q, Ma Q, et al. Transplantation of microbiota from drug-free patients with schizophrenia causes schizophrenia-like abnormal behaviors and dysregulated kynurenine metabolism in mice. *Mol Psychiatry.* 2020;25:2905–18.
84. Cryan JF, O'Riordan KJ, Cowan CS, Sandhu KV, Bastiaanssen TF, Boehme M, et al. The microbiota-gut-brain axis. *Physiol Rev.* 2019;99:1877–2013.
85. Guo X, Chen F, Gao F, Li L, Liu K, You L, et al. CNSA: a data repository for archiving omics data. *Database.* 2020;2020:baaa055.
86. Chen FZ, You LJ, Yang F, Wang LN, Guo XQ, Gao F, et al. CNGBdb: china national genebank database. *Yi Chuan.* 2020;42:799–809.

AUTHOR CONTRIBUTIONS

S.H., X.S. and J.L. designed the study; Participants were recruited by J.L., P.Z., J.J., H.H., C.X., L.W., X.G., Y.F., D.Z., Y.C., Y.Z., X.Y., X.L. and L.P.; J.L. and P.Z. coordinated the data processing and availability; Data analysis was performed as follows: serum metabolome

analysis (Z.L.), gut microbiota analysis (Z.L.) and neuroimaging analysis (J.D.); C.L., S.L., J.L., D.W., H.Z., M.H., H.Z., Y.S., L.W., Y.L., Z.J., S.L., W.Z. and H.Y. facilitated scientific discussion and gave suggestions; S.H., C.N., X.S. and K.K. supervised these activities; Z.L., J.D. and J.L. wrote the paper, which was revised by S.B., K.K. and S.H.; and all authors read and approved the manuscript.

FUNDING

This study was supported by grants from the National Natural Science Foundation of China (Grant numbers: 81971271 and 81971253), the Zhejiang Provincial Key Research and Development Programme (Grant number: 2021C03107), the Leading Talent of Scientific and Technological Innovation - 'Ten Thousand Talents Programme' of Zhejiang Province (Grant number: 2021R52016), the Zhejiang Provincial Natural Science Foundation (Grant number: LQ20H090013), the Programme from the Health and Family Planning Commission of Zhejiang Province (Grant number: 2020KY548) and Zhong yuan Technological Innovation leading Talents (Grant number: 204200510019).

CONFLICT OF INTEREST

The authors declare no competing interests.

ADDITIONAL INFORMATION

Supplementary information The online version contains supplementary material available at <https://doi.org/10.1038/s41380-022-01569-9>.

Correspondence and requests for materials should be addressed to Susanne Brix, Karsten Kristiansen, Xueqin Song, Chao Nie or Shaohua Hu.

Reprints and permission information is available at <http://www.nature.com/reprints>

Publisher's note Springer Nature remains neutral with regard to jurisdictional claims in published maps and institutional affiliations.